

Novel Features of the Main Transition of Dimyristoylphosphocholine Bilayers Revealed by Fluorescence Spectroscopy

Arimatti Jutila and Paavo K. J. Kinnunen*

Department of Medical Chemistry, Institute of Biomedicine, P.O. Box 8 (Siltavuorenpenger 10 A), FIN-00014, University of Helsinki, Finland

Received: April 25, 1997; In Final Form: June 17, 1997[⊗]

Lateral heterogeneity is evidenced in large unilamellar dimyristoylphosphatidylcholine vesicles by the transient peak at $T^* \approx 22^\circ\text{C}$ (approximately two degrees below the main transition temperature T_m) in intermolecular excimer formation by the pyrene-labeled phospholipid probe 1-palmitoyl-2-[10-(pyren-1-yl)]decanoyl-*sn*-glycero-3-phosphocholine (PPDPC). Using three different fluorescence quenchers, cholesteryl 22-(*N*-(7-nitrobenz-2-oxa-1,3-diazol-4-yl)amino)-23,24-bis(nor-5-chole-3 β -ol) (NBD-cholesterol), 1,2-dipalmitoyl-*sn*-glycero-3-phosphoethanolamino-*N*-(5-fluoresceinthiocarbonyl) (DPPF), and 1-palmitoyl-2-(*N*-4-nitrobenz-2-oxa-1,3-diazol)aminocaproylphosphocholine (NBD-PC) partitioning preferentially into the (i) phase boundary, (ii) gel phase, and (iii) fluid phase, respectively, we could demonstrate PPDPC at T^* to become weakly enriched into the interfacial boundary separating “fluid” domains from the bulk gel phase. Unexpectedly, at T_m there was a minimum in the colocalization of all three quenchers with PPDPC excimers. Our data are thus incompatible with the coexistence of fluid and gel state domains at T_m . Accordingly, the nature of the fluctuating entities underlying the heat capacity maximum at T_m must be reconsidered.¹ Phospholipid main transition is suggested to involve two transitions, from the gel state to an intermediate and from this intermediate state to the fluid state. Our data indicate the possibility that the intermediate phase in the vicinity of T_m is a strongly fluctuating “pseudocrystalline” superlattice of fluid (“excited”) and gel (“ground”) state lipids, with augmented short-range positional order of embedded impurities.

Introduction

One of the pertinent current questions regarding biomembrane function concerns the two-dimensional ordering of their components.² As most if not all biological membranes are believed to be in a fluid state under physiological conditions, it is of particular importance to establish mechanisms generating lateral heterogeneity and membrane ordering in this phase. Furthermore, as most cellular functions of eukaryotes apparently take place on membrane surfaces, elucidation of the coupling between organization and function of biomembranes is clearly of fundamental importance.³

Fluid–fluid immiscibility for some binary lipid alloys has been shown by DSC,⁴ Raman spectroscopy,⁵ and X-ray diffraction.⁶ On a mechanistic level hydrophobic mismatch of lipids has been demonstrated to result in the formation of microdomains in liquid crystalline bilayers.⁷ Likewise, reduction in water activity by poly(ethylene glycol) diminishes the size of the hydration shell of phospholipids, which then results in the enhancement of the contribution of the interactions between the hydrocarbon chains and causes phase separation.⁸ Fluorescence spectroscopy studies have indicated the formation of superlattices in fluid lipid membranes.^{9–13}

Characteristically of the liquid crystalline state of matter, biomembrane lipids exhibit a range of phases and phase transitions.¹⁴ The significance of these properties of lipids has mostly remained elusive. Phospholipid phase transitions could be important in regulating the activities of membrane-associated proteins.^{2,3,15–17}

Dynamic lateral heterogeneity due to coexisting fluctuating gel and liquid crystalline domains has been suggested to accompany the main transition of phospholipids.^{1,18–20} Upon

$T \rightarrow T_m$ the intensity of these fluctuations has been suggested to become enhanced and cause bending elasticity and lateral (area) compressibility as well as cause the heat capacity of the bilayer to have a maximum at T_m .^{1,19,21–23} The permeability maximum of bilayers and augmented activity of phospholipase A_2 near T_m ^{1,20,24–27} have been attributed to phase boundaries.²⁸ The length of the interfacial boundary has been predicted to have a maximum at T_m .¹⁹ Relaxation times measured by temperature jump,^{29–31} volume perturbation calorimetry,³² and ultrasonic absorption^{33–36} also have a maximum near T_m , indicating critical slowing down.^{37,38} Values of relaxation times in the range of hours following a thermal quench from fluid into the gel–fluid coexistence region have been reported.³⁹ The minimum in resonance energy transfer (RET) between NBD- and rhodamine-labeled 1,2-dipalmitoyl-PEs residing in DPPC (1,2-dipalmitoyl-*sn*-glycero-3-phosphocholine) was interpreted in terms of these probes differentially partitioning into coexisting gel and fluid domains at T_m .⁴⁰

We addressed the molecular level events of the main transition of 1,2-dimyristoyl-*sn*-glycero-3-phosphocholine (DMPC) using 1-palmitoyl-2-[10-(pyren-1-yl)]decanoyl-*sn*-glycero-3-phosphocholine (PPDPC). Photophysics of pyrene make this type of analog highly versatile.^{41,42} In brief, excited pyrene may either relax back to the ground state by emitting at ~ 400 nm or collide with a ground state pyrene so as to yield an excited dimer, excimer.⁴³ The latter relaxes back to two ground state pyrenes while emitting at ~ 480 nm. In the absence of possible quantum mechanical effects¹⁰ the ratio of excimer and monomer emission intensities (I_e/I_m) depends on the collision rate between pyrene moieties. Accordingly, pyrene-labeled lipids have been utilized to measure the rate of lateral diffusion of lipids⁴⁴ as well as the formation of domains^{7,45} and superlattices^{9–13} in membranes.

Complementing the I_e/I_m data for PPDPC in DMPC, we also utilized a two-probe method measuring resonance energy

* To whom all correspondence should be addressed. Telephone: 358-9-1918237. Fax: 358-9-1918276. E-mail: Paavo.Kinnunen@Helsinki.Fi.

[⊗] Abstract published in *Advance ACS Abstracts*, August 15, 1997.

transfer between PPDPC and three different acceptors for pyrene excimer emission, NBD-chol, DPPF, and NBD-PC, in order to determine changes in the preferential location of PPDPC in the course of the main transition.

Experimental Procedures

Materials. Cholesterol, Hepes, and EDTA were from Sigma. PPDPC was from K&V Bioware (Espoo, Finland), NBD-PC was from Avanti Polar Lipids (Alabaster, AL), and DPPF and NBD-chol were from Molecular Probes (Eugene, OR). No impurities were detected in the above lipids upon thin-layer chromatography on silicic acid using chloroform/methanol/water/ammonia (65:20:2:2, by volume) as the solvent system and examination of the plates for pyrene fluorescence or after iodine staining. The concentration of DMPC (Princeton Lipids, Princeton, NJ) was determined by phosphorus assay⁴⁶ and that of cholesterol gravimetrically. Concentrations of the fluorescent lipids were determined spectrophotometrically. For PPDPC absorption was measured at 342 nm, and 42,000 cm⁻¹ was used as the molar extinction coefficient. For DPPF 75,000 cm⁻¹ at 497 nm, for NBD-chol 22,000 cm⁻¹ at 465 nm, and for NBD-PC 21,000 cm⁻¹ at 465 nm were employed. Water was freshly deionized in a Milli RO/Milli Q (Millipore) filtering system.

Preparation of Liposomes. Samples were prepared by dissolving and mixing the indicated lipids in chloroform to obtain the desired compositions, whereafter the solvent was removed under a stream of nitrogen. The residues were subsequently maintained under reduced pressure for at least 2 h and then hydrated at 37 °C to yield a lipid concentration of 1 mM. To obtain large unilamellar vesicles (LUV), the hydrated lipid mixtures were extruded with a LiposoFast small-volume homogenizer (Avestin, Ottawa, Canada), subjecting the lipid dispersions to 19 passes through two polycarbonate filters (100 nm pore size, Nucleopore, Pleasanton, CA) installed in tandem. All samples were annealed by taking them five times through the transition by repeated heating and cooling between 0 and 37 °C, whereafter they were stored at 4 °C overnight. Final total concentration of phospholipid was 25 μM in 20 mM Hepes–0.1 mM EDTA buffer, pH 7.0 (adjusted with NaOH). All temperature scans were performed by increasing the temperature in 0.2–1.0 °C steps from 11 to 30 °C, the average heating rate being ~0.07 °C/min in the temperature range between 20 and 25 °C.

Fluorescence Spectroscopy. Fluorescence measurements were carried out with a Perkin Elmer LS50B spectrometer interfaced to a Compaq 486 Prolinea 4/25s computer. Cuvette temperature was controlled by a circulating water bath, and the contents were continuously agitated by a magnetic stirring bar. PPDPC was excited at 344 nm, and monomer and excimer emission intensities were detected at 398 and 480 nm, respectively. For samples with $X_{\text{PPDPC}} = 0.02$ or 0.03 (X = mole fraction) bandwidths of 3.0 nm were used. Otherwise band-passes of 4.0 nm were employed. Due to the low concentrations of the chromophores used, minimal inner filter effect is expected. When indicated, two fluorescent probes were simultaneously present in the LUVs. More specifically, PPDPC was used as a RET donor, while either NBD-chol, NBD-PC, or DPPF was employed as an acceptor.

Differential Scanning Calorimetry. Differential heat capacity scans were recorded with a Privalov high-sensitivity adiabatic differential scanning instrument (DASM-4, Biopribor, Puschino, Russia) at a lipid concentration of 0.7 mM (heating rate of 0.5 °C/min). The calorimeter was interfaced to a 486 PC via a DT01-EZ data acquisition board (Data Translation, Marlboro, MA), and data were analyzed using the routines of the Origin software (Microcal, Northampton, MA).

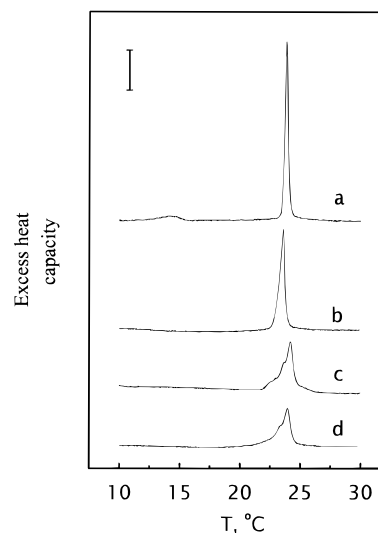


Figure 1. Differential scanning calorimetry (DSC) of multilamellar vesicles (MLV) of DMPC and DMPC/PPDPC (99:1, molar ratio, traces a and b, respectively) and the corresponding LUVs (traces c and d) recorded after extrusion of the MLVs through polycarbonate filters. The calibration bar corresponds to 5 kJ / °C mol⁻¹.

TABLE 1: Comparison of the Main Transition Temperatures and Enthalpies for Multilamellar (MLVs) and Large Unilamellar Vesicles (LUVs) Having the Indicated Compositions

	T_m , °C		ΔH_m , kJ/mol	
	MLV	LUV	MLV	LUV
DMPC	23.8	24.1	25.4	25.0
PPDPC/DMPC (1:99)	23.6	23.9	22.3	18.1
PPDPC/DMPC (2:98)	23.3	24.1	25.3	20.3
PPDPC/DMPC (3:97)	23.5	23.4	24.0	19.0
PPDPC/NBD-chol/DMPC (1:1:98)	23.4	23.8	31.6	21.9
PPDPC/DPPF/DMPC (1:1.6:97.4)	23.6	24.1	26.8	19.9
PPDPC/NBD-PC/DMPC (1:1:98)	23.5	23.9	28.2	23.6

Unlike DMPC MLVs (multilamellar vesicles), which are routinely used in DSC, LUVs composed of this phospholipid lack the pretransition and exhibit a single endotherm at ~24.1 °C with a total enthalpy of ~25.0 kJ/mol (Figure 1). The amounts of the probes used in the fluorescence measurements did not influence the shape of the main transition peak. Yet, they slightly altered the main transition temperature T_m and also abolished the pretransition peak observed for DMPC MLVs at ~14 °C. These data are compiled in Table I. The small shoulder in the main endotherm of LUVs coincides with the main transition temperature for the original MLVs and is likely to be due to the presence of a small contaminating population of MLVs, having diameters equal to or smaller than the 100 nm pore size of the filters used. Removal of the MLVs would have been extremely difficult, for the following reasons. As these MLVs have passed through the 100 nm pore size filters, they would not separate upon gel permeation chromatography from the LUVs. Shifting of density would have necessitated the exposure of the vesicles to osmotic pressure gradients. Our previous investigations have shown osmotic pressure to exert significant effects on lipid packing which, in turn, causes marked signals to be obtained from the type of pyrene-labeled lipid probe used in this study.⁸

Results

Only a smooth monotonic increase in I_e/I_m vs T has been so far observed for PPDPC residing in DMPC liposomes.^{8,47} At higher resolution, however, a transient peak in I_e/I_m is evident

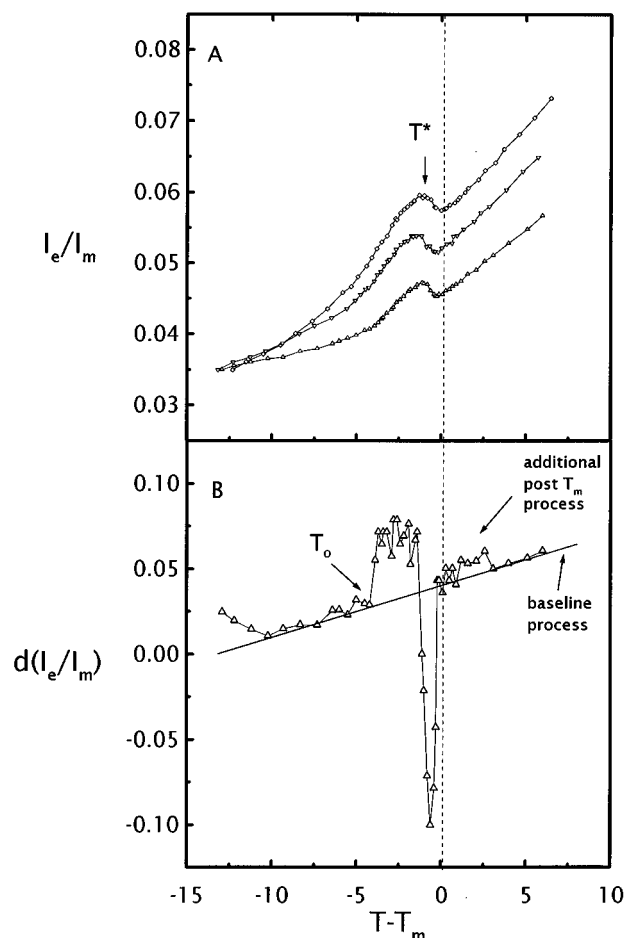


Figure 2. (A) I_e/I_m vs $T - T_m$ for PPDPC residing in large unilamellar vesicles (LUV) of DMPC at X_{PPDPC} of either 0.01 (Δ), 0.02 (∇), or 0.03 (\diamond). (B) First derivative of I_e/I_m vs $T - T_m$ for liposomes at $X_{PPDPC} = 0.01$. T_0 denotes the temperature where the values for I_e/I_m below T_m start to deviate from the slowly ascending baseline. T^* denotes the temperature where the transient peak in I_e/I_m has its maximum.

(denoted by T^* , Figure 2A), preceding the specific heat peak at $T_m \approx 23.9$ °C, determined for these LUVs by DSC (Figure 1). First derivative $d(I_e/I_m)$ vs $(T - T_m)$ reveals a "baseline process" which progressively enhances I_e/I_m , while there is a transient increase in I_e/I_m beginning (at T_0) at ~ 4 °C below T_m and reaching a maximum at ~ 2 °C below T_m (Figure 2B). At T_m the I_e/I_m values return close to the ascending baseline attributed to the thermally enhanced excimer formation. Yet, $d(I_e/I_m)$ vs $(T - T_m)$ also shows a weaker process when $T > T_m$, which is complete at ~ 2 °C above T_m . Increasing X_{PPDPC} (mole fraction of PPDPC) increases the deflection in I_e/I_m at T^* (Figure 2A), and compared to $X_{PPDPC} = 0.01$ the integrated area of the peak is ~ 1.4 - and 2.5 -fold at $X_{PPDPC} = 0.02$ and 0.03 , respectively. The transient increment in I_e/I_m below T_m could be due to lateral enrichment of the probe or enhanced lateral diffusion. As "fluidity" and lateral diffusion are augmented upon exceeding T_m , lateral enrichment seems more plausible.

Upon approaching T_m , formation of "fluid" domains should ensue within the gel bulk.^{1,18–20} To distinguish between the enrichment of PPDPC into the (i) gel phase, (ii) fluid domains, or (iii) domain interface, we utilized additional fluorescent lipids selected by two criteria. First, their spectral properties should allow them to function as resonance energy transfer (RET) acceptors for PPDPC excimer emission, and second, they should have different solubilities in the different lipid phases. Colocalization parameter C was then defined as

$$C = (I_0 - I)/I_0$$

where I_0 and I are emission intensities measured for PPDPC in the absence and presence of the acceptor, respectively. Maximum ($I \rightarrow 0$) for C indicates augmented colocalization of the probes, whereas minimum ($I \rightarrow I_0$) reports the probes being dispersed in the membrane. Importantly, quantitative analysis of the resonance energy transfer data is ambiguous due to the lack of information on the orientation of the oscillating dipoles of the fluorophores and uncertainty concerning probe distribution.⁴⁹ This drawback, however, does not jeopardize the qualitative conclusions of the present study. Furthermore, due to the extensive and, compared to the fluorescence lifetimes, very rapid thermal motion of the chromophores, it is highly unlikely that the mutual orientation of the oscillating dipoles would limit the efficiency of RET. Accordingly, changes in RET can be readily expected to be mostly determined by changes in the average distances between the donor and acceptor.

Cholesterol reduces line tension between coexisting solid and fluid domains and favors partitioning into the interface.^{20,50,51} Accordingly, 22-(*N*-(7-nitrobenz-2-oxa-1,3-diazol-4-yl)amino)-23,24-bis(nor-5-chole-3 β -ol) (NBD-cholesterol, at $X = 0.01$), i.e. a cholesterol analog containing a covalently linked NBD-fatty acid moiety, was first employed as an acceptor. At $X = 0.01$ the parent compound cholesterol did not affect the peak in I_e/I_m for PPDPC to any measurable extent (data not shown). Likewise, T_m remained nearly unaffected by these probes and was measured by DSC at 23.9 and 23.8 °C for both PPDPC/DMPC (1:99, molar ratio) and PPDPC/NBD-cholesterol/DMPC (1:1:98) LUVs, respectively. A minor decrease in T_m (~ 0.1 °C) was measured for MLVs containing also NBD-cholesterol.

The influence of NBD-cholesterol on the temperature dependency of I_e/I_m was dramatic (Figure 3A). Values for I_e/I_m increase progressively with temperature, and the peak at T^* is lacking. The fact that I_e/I_m is increased in the presence of NBD-cholesterol is likely to reflect more efficient quenching of pyrene monomer species by this acceptor. At this stage it is impossible to distinguish if this (i) is due to transient colocalization of NBD-cholesterol and PPDPC (in monomer state) over the whole temperature range studied or (ii) simply reflects more efficient coupling of the dipoles of excited monomeric PPDPC and NBD-cholesterol. C vs $(T - T_m)$ reveals colocalization in the gel phase to diminish with the first minimum at ~ 5 °C below T_m (Figure 3D). Thereafter a peak in colocalization is evident at T^* , subsequently followed by a minimum at $\sim T_m$. Upon further increase in temperature above T_m , there is a slight increase in C . Assuming NBD-cholesterol to favor partitioning into the gel–fluid interface similarly to cholesterol, our data strongly suggest the peak in I_e/I_m for PPDPC at T^* to result from preference of this probe for the domain boundary.

We subsequently utilized 1,2-dipalmitoyl-*sn*-glycero-3-phosphoethanolamino-*N*-(5-fluorescein-thiocarbonyl) (DPPF) as a quencher for pyrene excimer.^{7,52} The long saturated acyl chains of DPPF can be readily anticipated to favor partitioning of this probe into the gel phase. In keeping with this, DSC revealed DPPF ($X = 0.016$) to slightly increase T_m (from 23.9 to 24.1) of DMPC LUVs containing PPDPC ($X = 0.01$), i.e. to weakly stabilize the gel phase (Table 1). A similar result was obtained when X_{DPPF} was increased to 0.04 (data not shown). This contrasts the effect of DPPF in DPPC LUVs, i.e. in a matrix with identical acyl chains, where significant decrease in T_m was observed.⁴⁰ Although DPPF suppresses I_e/I_m over the entire temperature interval investigated, the peak at T^* remains nearly unaffected (Figure 3B). This indicates that at T^* DPPF is

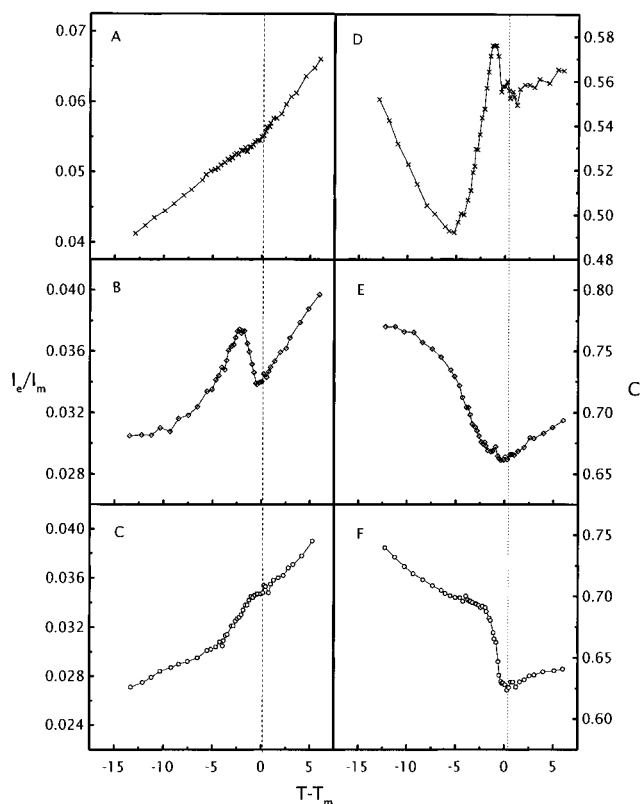


Figure 3. Values for I_e/I_m vs $T - T_m$ for DMPC LUVs incorporating PPDPC ($X = 0.01$) together with either NBD-cholesterol ($X = 0.01$, A), DPPF ($X = 0.016$, B), or NBD-PC ($X = 0.01$, C). Colocalization parameter C vs $T - T_m$ calculated for the respective PPDPC-acceptor pairs, i.e. with NBD-cholesterol (D), DPPF (E), and NBD-PC (F).

localized neither into the domains enriched in PPDPC nor in their immediate vicinity. C vs $(T - T_m)$ demonstrates colocalization of DPPF and PPDPC to decrease when $T \rightarrow T^*$, whereafter a minimum follows at T_m (Figure 3E). Above T_m colocalization of the chromophores is augmented. To conclude, the above data suggest colocalization of DPPF and PPDPC to decrease when the latter becomes enriched into the fluid-gel interface while DPPF remains in the gel domains.

To complement our approach, we then used 1-palmitoyl-2-(*N*-4-nitrobenz-2-oxa-1,3-diazol)aminocaproylphosphocholine (NBD-PC) as a RET acceptor. In lipid monolayers residing on an air/water interface NBD-PC partitions into fluid domains.⁵⁰ The measured I_e/I_m vs $(T - T_m)$ as well as C vs $(T - T_m)$ are both intermediate between those for NBD-cholesterol and DPPF (Figure 3F). The slow decrease in C when $T \rightarrow T^*$ as well as its more abrupt decline slightly below T_m is compatible with dissolving of microscopic domains enriched in both probes. The most likely reason for the formation of such microdomains when $T \ll T_m$ is minimizing free energy by reduction in the extent of perturbation of the packing of the gel state DMPC matrix. Following a minimum in C at T_m , there is a slight increase in RET between the two probes, coinciding with the temperature range of the post-transition process (Figure 2B).

Discussion

The present results provide evidence for lateral heterogeneity in DMPC LUVs below the main transition temperature. More specifically, a transient peak in I_e/I_m is observed for the fluorescent probe, PPDPC, at $T = T^*$, ~ 2 °C below the T_m for the LUVs. Our DSC measurements indicate a small population of MLVs to be present in the LUVs obtained by the extrusion technique. As the T_m for MLVs was maximally ~ 0.5 °C lower

than for the corresponding LUVs, the contaminating MLVs as a source for the peak in I_e/I_m can be excluded. To this end, we are at present unable to provide an unambiguous explanation for the higher T_m values for LUVs (Figure 1 and Table 1). One possibility could be thermal expansion. In brief, upon increase in temperature, the expansion of the inner bilayer shells in MLVs exerts pressure on the outer bilayers, thus causing their lateral expansion and weaker chain-chain interactions. Due to cooperativity, the whole MLV would therefore melt at a lower temperature than the corresponding LUV. Broadening of the main transition endotherms in LUVs reflects decreased cooperativity of the membrane arising from (i) smaller size of the vesicles limiting the maximum size of the cooperative unit and/or (ii) the effect of increased curvature of the vesicles.¹⁸

Our resonance energy transfer data support the view that the transient peak in I_e/I_m at T^* originates from a fraction of PPDPC in the membrane partitioning into the interfacial boundary separating "fluid" domains from the gel bulk below T_m . Except for this preference for the boundary, PPDPC appears to represent a minor perturbant to the DMPC matrix, diffusing with similar constraints in both gel and liquid crystalline phases as well as at T_m . The driving forces for the enrichment of PPDPC into the interface between "fluid" and gel domains below T_m can be rationalized as follows. As a substitutional impurity PPDPC perturbs the gel state lattice and it can be anticipated to be repelled, although weakly, from this matrix, similarly to the exclusion of this probe from the gel state of DPPC.⁹ Upon main transition, there is a $\sim 20\%$ reduction in bilayer thickness and $\sim 20\%$ lateral area expansion.⁵³ As the effective length of PPDPC exceeds the thickness of fluid DMPC,⁷ hydrophobic mismatch opposes the partitioning of the probe also into the fluid phase. While increase in free energy due to hydrophobic mismatch between PPDPC and gel state DMPC should be less than that between PPDPC and fluid phase DMPC, the perturbation by PPDPC of the packing of DMPC in the gel state is more severe than that imposed by the probe on the packing of fluid phase DMPC. A free energy minimum appears to be achieved when a fraction of PPDPC is localized into the "fluid"/gel boundary, thus resulting in a local enrichment of the probe. This further causes augmented collision frequency between the PPDPC probes in this domain and thus enhances I_e/I_m .

The boundaries between the different phases are not exact, sharp lines, but gradients in which the rate and the extent of *trans* \rightarrow *gauche* isomerization change.⁵¹ In accordance, phase boundaries are "soft" and easily accommodate impurities.²⁰ However, there must also be a process that restricts the accumulation of the probe into the domain interface. We as well as others have provided evidence for steric perturbation of fluid lipid matrices by PPDPC to cause a repulsive potential between the probes.⁹⁻¹² This repulsive potential could be strong enough to limit the partitioning of PPDPC into the boundary. As shown in Figure 2, increasing X_{PPDPC} increases also the intensity of the peak in I_e/I_m at T^* . Therefore, the partitioning of PPDPC into the boundary represents chemical equilibrium. To this end, reasoning similar to that described above for PPDPC could also be applicable so as to explain the mechanism causing the preference of cholesterol for the fluid/gel domain boundaries. The fact that cholesterol ($X = 0.01$) as such had essentially no effect on the I_e/I_m vs T scans suggests that this amount of cholesterol has no major influence on the partitioning of PPDPC within the bilayer and/or on the collision frequency of PPDPC within the phase boundary. Not excluding the above mechanisms it could also be that cholesterol at $X = 0.01$ does not have any measurable influence on the length of the fluid/gel boundary. This would indicate that the phase transition process

would be determined by DMPC. At this stage of our investigation it is not possible to distinguish between the above alternatives.

Our data further indicate that the formation of "fluid" domains and the "fluid"/gel (f/G) interface starts at $\sim T_0 \approx 20^\circ\text{C}$, well below T_m (Figure 2B). This temperature coincides with the ultrasound absorption for DMPC bilayers.⁵⁴ The weak enrichment of PPDPC into the boundary should commence at T_0 and thus result in an increase in I_e/I_m . Upon increase in T in the interval $T_0 < T < T^*$, the length $l_{f/G}$ of the boundary increases with further increase in I_e/I_m due to a larger number of PPDPC becoming accommodated into the interface.

Boundaries between regions with incommensurate packing properties increase the total free energy, therefore tending to minimize the length of the interface and thus preferring larger entities instead of a number of small ones. Upon approaching T_m , the fraction of "fluid" area increases and at some temperature the domains coalesce. Importantly, the position of the peak in I_e/I_m at T^* with respect to T_m is not shifted to higher temperatures when X_{PPDPC} is increased. This observation contradicts the view that the decrease in I_e/I_m upon T increasing from T^* to T_m would be due to the dilution of the probe, caused by an increase in the length of the boundary. Instead, the constant value for $T^* - T_m$ at increasing content of PPDPC is compatible with the interpretation of the boundary length having a maximum at T^* , whereafter the decline of the peak in I_e/I_m would report decreasing length of the "fluid"/gel boundary. Notably, T^* is close to the critical temperature measured for shear relaxation by ultrasound⁵⁴ in further keeping with the notion that below T^* there are "fluid" domains in gel bulk, whereas at T^* the former becomes the continuous phase.

Above T_m the minor deviation from the baseline evident in $d(I_e/I_m)/dT$ ($T - T_m$) suggests that PPDPC is very weakly enriched also into the phase boundary between "gel" domains in fluid bulk. Importantly, the physical properties of "fluid" domains in the gel state bilayer below T_m are not identical to those of the fluid bulk above T_m . This is understandable as upon increase in T , the extent of *trans* \rightarrow *gauche* isomerization of the acyl chains in fluid domains further increases, fluid domains becoming "more fluid". Simultaneously, also the properties of the remaining gel phase change in an analogous manner, and the physical properties of the "gel"-like domains in the fluid bilayer above T_m are not representative of the gel state below T_m . Accordingly, the properties of the boundaries between "fluid" domains in gel bulk ($T < T_m$) and "gel" domains in fluid bulk ($T > T_m$) must be different.

A number of studies have reported anomalies in membrane properties either below or above T_m .^{26,34,54-56} Our data indicate microdomain formation below and perhaps also above T_m . Importantly, at T_m and on the time scale of the lifetime of the pyrene excimer (on the order of 10^{-8} s)⁴⁷ there appears to be no gel or fluid DMPC domains and no real phase boundaries. Instead, the boundary appears to vanish completely, as indicated by (i) I_e/I_m and by (ii) a minimum in C at T_m for all three quenchers. The latter data reveal that there is a maximum in the average distances between PPDPC excimers and the different acceptors at T_m during the lifetime of the pyrene excimer. The lack of boundaries necessitates the nature of the fluctuating entities underlying the maximum in heat capacity at T_m .^{1,19,20} to be reconsidered. Our data would be consistent with the main transition involving two subsequent transitions in the vicinity of T_m : gel \leftrightarrow intermediate and intermediate \leftrightarrow fluid, as follows. With increasing temperature the number of defects (i.e. lipids with acyl chains in *gauche* conformation) in the gel state lattice first increases well below T_m .⁵⁷ Formation of the "fluid"

domains in gel phase bulk by these excited state lipids commences at T_0 and results in increased ultrasound absorption⁵⁴ as well as in the augmented I_e/I_m for the fluorescent lipid, PPDPC, due to the weak enrichment of this probe into the domain boundaries. The "fluid" domains subsequently increase in their size and number. At T^* the length of the interfacial boundary, $l_{f/G}$, reaches its maximum. Close to T^* the "fluid" domains coalesce and form a continuous phase. Subsequently, the boundary length begins to decrease. Upon further increase in temperature the transition is not directly from the gel into the fluid phase, however, and these phases are separated by an intermediate phase existing at temperatures close to T_m . Accordingly, at proper thermal excitation ($T^* < T < T_m$) domains of "fluid" and gel state molecules merge into a highly cooperative lattice. To some extent this represents a situation where the entire bilayer has the properties of a fluctuating gel/fluid interface. Within a narrow temperature interval centered at T_m the bilayer would thus consist of a fluctuating, extremely cooperative superlattice of regularly distributed "fluid" state phospholipids, ideally forming at T_m a lattice of 1:1 stoichiometry with "gel" state phospholipids.³ The conformational states of the lipids in these lattices would be fully exchangeable and would require cooperative transfer of quanta from excited ("fluid") state lipids to ground ("gel") state lipids so as to obtain an increase of the degree of *trans* \rightarrow *gauche* isomerization of the acyl chains of the latter and decrease in the former. The distribution and exchange of energy states of the lipids would be highly correlated with the coherence length approaching infinity at T_m .³⁸ These thermally maintained long-range coherent oscillations (standing waves, "oscillons")⁵⁸ would cause the rate of lateral diffusion of the quenchers (impurities) to decrease, as due to their different chemical structure, they cannot exchange quanta with the matrix lipid. In other words this slowing down of lateral diffusion of the quenchers at T_m would be due to the free energy minimum of the system requiring highly cooperative coupling of the energy states of neighboring lipids, which further would be perturbed by the quenchers. In time domain, this perturbation is diminished by limiting the lateral diffusion of the impurities; that is, at T_m they are trapped within the strongly fluctuating superlattice. This would be evident as their augmented short-range positional order at T_m . Above T_m transition from the intermediate phase to "gel" domains in fluid bulk takes place. Upon further increase in T , the size and number of the "gel" domains decrease, the entire membrane becoming fluid.

The above model somewhat resembles phase transition of liquid crystals having the hexatic phase involved in the melting of two-dimensional solids described as a two-step process, the phases slightly below and above T_m being similar on a microscopic scale.^{59,60} The phase transition of biomembrane phospholipids would thus not be totally unlike other two-dimensional melting processes.⁶¹

Acknowledgment. One of us (P.K.) is grateful to Prof. Ole G. Mouritsen (Technical University of Denmark, Lyngby) for several rewarding discussions on the data. Work in our laboratory is supported by Finnish State Medical Research Council and Biocenter Helsinki.

References and Notes

- (1) Doniach, S. *J. Chem. Phys.* **1978**, *68*, 4912.
- (2) Mouritsen, O. G.; Kinnunen, P. K. *J. Biological Membranes*; Merz, K. M., Jr., Roux, B., Eds.; Birkhäuser Publishing: Boston, 1996; pp 465-504.
- (3) Kinnunen, P. K. *J. Chem. Phys. Lipids* **1991**, *57*, 357.
- (4) Melchior, D. L. *Science* **1986**, *234*, 1577.
- (5) Litman, B. J.; Lewis, E. N.; Levin, I. W. *Biochemistry* **1991**, *30*, 313.

- (6) Hinderliter, A. K.; Huang, J.; Feigenson, G. W. *Biophys. J.* **1994**, 67, 1906.
- (7) Lehtonen, J. Y. A.; Holopainen, J. M.; Kinnunen, P. K. J. *Biophys. J.* **1996**, 70, 1753.
- (8) Lehtonen, J. Y. A.; Kinnunen, P. K. J. *Biophys. J.* **1995**, 68, 525.
- (9) Somerharju, P. J.; Virtanen, J. A.; Eklund, K. K.; Vainio, P.; Kinnunen, P. K. J. *Biochemistry* **1985**, 24, 2773.
- (10) Kinnunen, P. K. J.; Tulkki, A.-P.; Lemmetyinen, H.; Paakkola, J.; Virtanen, J. A. *Chem. Phys. Lett.* **1987**, 136, 539.
- (11) Tang, D.; Chong, P. L.-G. *Biophys. J.* **1992**, 63, 903.
- (12) Chong, P. L.-G.; Tang, D.; Sugar, I. P. *Biophys. J.* **1994**, 66, 2029.
- (13) Tang, D.; van der Meer, B. W.; Chen, S.-Y. S. *Biophys. J.* **1995**, 68, 1944.
- (14) Kinnunen, P. K. J.; Laggner, P., Eds. Special Issue of *Chem. Phys. Lipids* **1991**, 57, 109.
- (15) Kinnunen, P. K. J.; Mouritsen, O. G., Eds. Special Issue of *Chem. Phys. Lipids* **1994**, 73, 1.
- (16) Tocanne, J.-F.; Cézanne, L.; Lopez, A.; Piknova, B.; Schram, V.; Tournier, J.-F.; Welby, M. *Chem. Phys. Lipids* **1994**, 73, 139.
- (17) Epand, R., Ed. Special Issue of *Chem. Phys. Lipids* **1996**, 81, 101.
- (18) Marsh, D.; Watts, A.; Knowles, P. F. *Biochim. Biophys. Acta* **1977**, 465, 500.
- (19) Freire, E.; Biltonen, R. *Biochim. Biophys. Acta* **1978**, 514, 54.
- (20) Mouritsen, O. G.; Jørgensen, K.; Hønger, T. *Permeability and Stability of Lipid Bilayers*; Disalvo, E. A., Simon, S. A., Eds.; CRC Press: Boca Raton, FL, 1995; pp 137–160.
- (21) Nagle, J. F.; Scott, H. L. *Biochim. Biophys. Acta* **1978**, 513, 236.
- (22) Evans, E.; Kwok, R. *Biochemistry* **1982**, 21, 4874.
- (23) Bloom, M.; Evans, E.; Mouritsen, O. G. *Q. Rev. Biophys.* **1991**, 24, 293.
- (24) Papahadjopoulos, D.; Jacobson, K.; Nir, S.; Isac, T. *Biochim. Biophys. Acta* **1973**, 311, 330.
- (25) Op den Kamp, J. A. F.; Kauertz, M. T.; Van Deenen, L. L. M. *Biochim. Biophys. Acta* **1975**, 406, 169.
- (26) Maynard, V. M.; Magin, R. L.; Dunn, F. *Chem. Phys. Lipids* **1985**, 37, 1.
- (27) Menashe, M.; Romero, G.; Biltonen, R. L.; Lichtenberg, D. J. *Biol. Chem.* **1986**, 261, 5328.
- (28) Hønger, T.; Jørgensen, K.; Biltonen, R. L.; Mouritsen, O. G. *Biochemistry* **1996**, 35, 9003.
- (29) Tsong, T. Y.; Kanehisa, M. I. *Biochemistry* **1977**, 16, 2674.
- (30) Kanehisa, M. I.; Tsong, T. Y. *J. Am. Chem. Soc.* **1978**, 100, 424.
- (31) Gruenewald, B.; Frisch, W.; Holzwarth, J. F. *Biochim. Biophys. Acta* **1981**, 641, 311.
- (32) Van Osdol, W. W.; Johnson, M. L.; Ye, Q.; Biltonen, R. L. *Biophys. J.* **1991**, 59, 775.
- (33) Mitaku, S.; Ikegami, A.; Sakanishi, A. *Biophys. Chem.* **1978**, 8, 295.
- (34) Mitaku, S.; Jippo, T.; Kataoka, R. *Biophys. J.* **1983**, 42, 137.
- (35) Harkness, J. E.; White, R. D. *Biochim. Biophys. Acta* **1979**, 552, 450.
- (36) Mitaku, S.; Okano, K. *Biophys. Chem.* **1981**, 14, 147.
- (37) Mitaku, S.; Date, T. *Biochim. Biophys. Acta* **1982**, 688, 411.
- (38) Careri, C. *Order and Disorder in Matter*; The Benjamin/Cummings Publishing Co: Menlo Park, 1984.
- (39) Jørgensen, K.; Klinger, A.; Braiman, M.; Biltonen, R. L. *J. Phys. Chem.* **1996**, 100, 2766.
- (40) Pedersen, S.; Jørgensen, K.; Bækmark, T. R.; Mouritsen, O. G. *Biophys. J.* **1996**, 71, 554.
- (41) Kinnunen, P. K. J.; Kõiv, A.; Mustonen, P. *Fluorescence Spectroscopy*; Wolfbeis, O. S., Ed.; Springer-Verlag: Berlin, 1993; pp 159–171.
- (42) Duportail, G.; Lianos, P. *Vesicles*; Rosoff, M., Ed.; Marcel Dekker: New York, 1996; pp 296–372.
- (43) Förster, Th. *Angew. Chem., Int. Ed. Engl.* **1969**, 8, 333.
- (44) Galla, H.-J.; Theilen, U.; Hartmann, W. *Chem. Phys. Lipids* **1979**, 23, 239.
- (45) Eklund, K. K.; Vuorinen, J.; Mikkola, J.; Virtanen, J. A.; Kinnunen, P. K. J. *Biochemistry* **1988**, 27, 3433.
- (46) Bartlett, G. R. *J. Biol. Chem.* **1959**, 234, 466.
- (47) Hresko, R. C.; Sugár, I. P.; Barenholz, Y.; Thompson, T. E. *Biochemistry* **1986**, 25, 3813.
- (48) Lange, Y. *The Physical Chemistry of Lipids: From Alkanes to Phospholipids*; Small, D. M., Ed.; Plenum Press: New York, 1986; pp 523–554.
- (49) Drake, J. M.; Klafter, J.; Levitz, P. *Science* **1991**, 251, 1574.
- (50) Weis, R. M.; McConnell, H. M. *J. Phys. Chem.* **1985**, 89, 4453.
- (51) Hwang, J.; Tamm, L. K.; Böhm, C.; Ramalingam, T. S.; Betzig, E.; Edidin, M. *Science* **1995**, 270, 610.
- (52) Kõiv, A.; Palvimo, J.; Kinnunen, P. K. J. *Biochemistry* **1995**, 34, 8018.
- (53) Wilkinson, D. A.; Nagle, J. F. *Liposomes: From Physical Structure to Therapeutic Applications*; Knight, C. G., Ed.; Elsevier/North-Holland Biomedical Press: Amsterdam, 1981; pp 273–297.
- (54) Eggers, F.; Funck, T. *Naturwissenschaften* **1976**, 63, 280.
- (55) Wu, E.-S.; Jacobson, K.; Papahadjopoulos, D. *Biochemistry* **1977**, 16, 3936.
- (56) Fernandez-Puente, L.; Bivas, I.; Ditov, M. D.; Méléard, P. *Europhys. Lett.* **1994**, 28, 181.
- (57) Kosterlitz, J. M.; Thouless, D. J. *J. Phys. C: Solid State Phys.* **1973**, 6, 1181.
- (58) Umbanhowar, P. B.; Melo, F.; Swinney, H. L. *Nature* **1996**, 382, 793.
- (59) Halperin, B. I.; Nelson, D. R. *Phys. Rev. Lett.* **1978**, 41, 121.
- (60) Brinkman, W. F.; Fisher, D. S.; Moncton, D. E. *Science* **1982**, 217, 693.
- (61) Bruinsma, R. *Nature* **1989**, 341, 486.